Energy & Buildings 289 (2023) 113047

Contents lists available at ScienceDirect

Energy & Buildings

journal homepage: www.elsevier.com/locate/enb

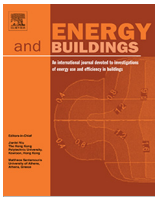

Two-stage evaporator for R744 heat pumps using greywater as heat source

Ángel Á. Pardiñas [a,*], Hanne Kauko [a], Mihir Mouchum Hazarika [b], Håkon Selvnes [a], Krzysztof Banasiak [a], Armin Hafner [b]

[a] SINTEF Energi AS, Trondheim 7034, Norway
[b] Norwegian University of Science and Technology, Trondheim 7491, Norway

ARTICLE INFO

Article history:
Received 29 September 2022
Revised 27 December 2022
Accepted 2 April 2023
Available online 7 April 2023

Keywords:
Heat pump
Carbon dioxide
R744
Greywater
Wastewater
Heat exchanger
Evaporator
Ejector

ABSTRACT

Heat pumps are pinpointed as a key technology in decarbonizing buildings' heat supply, which is currently dominated by fossil-fuel based systems. To minimize the environmental impact of heat pumps over their lifetime, selecting natural working fluids (refrigerants) is the only viable long-term choice. Independent of the refrigerant, the efficiency of a heat pump is closely linked to temperature of the applied heat source, and to this end, wastewater is a promising candidate that is abundant in all urban environments. This experimental study investigates a novel two-stage, ejector-supported, brazed plate evaporator for its use in R744 (CO_2) heat pumps with greywater as a heat source and compares it to more conventional evaporators. The work shows that splitting the evaporation process in two stages with an ejector in between allows reducing the evaporation pressure while the compressor suction pressure can be increased, in some cases significantly. Even if several possibilities for further optimization of the novel two-stage evaporator were identified, the results show heat pump efficiency improvements above 10 % compared to an equivalent heat pump with a well-performing one-stage evaporator. Heat pump systems aiming at utilizing maximum temperature difference for the greywater should use a high pressure lift ejector.

1. Introduction

The building sector is responsible for about 30 % of the global energy consumption and nearly 15 % of direct CO_2 emissions [1,2]. The current trend towards better insulated houses or even passive houses involves that the share of hot water production in the total energy demand in buildings is increasing [3]. Thus, more emphasis needs to be put in efficient production of domestic hot water (DHW). To this end, there is a great potential in the wastewater exergy content in the housing and commercial sectors: 80 to 90 % of the original thermal energy of hot water is sent to the drain as greywater [4]. According to Frijns et al. [5], the average temperature of domestic wastewater is 27 °C, which is still very interesting for several applications. Wastewater in domestic and commercial sectors can be classified into greywater, coming from showers, WC basins and bathtubs and with lower to medium concentration of waste contents, and blackwater, coming from toilets and bidets, at relatively low temperature and with very high contents of residues (faeces, urine, toilet paper) [6]. Conventionally, the different streams are combined, meaning that very different temperature levels and compositions within the wastewater are mixed altogether for simplicity and reducing the amount of pipework in the building. However, newer buildings (including passive houses) should account for separation of the different wastewater streams. This was evaluated e.g. in [3] for a heat pump application (wastewater as heat source), proving that the COP is higher when only the wastewater coming from showers was utilized compared to retrieving heat from all the wastewater streams combined.

Decarbonizing the heating and cooling demand in the building sector by electrification is regarded as a key measure to reduce emissions [7,8], and the role of heat pumps in this new energy scenario is undisputed. In this context, widespread use of wastewater as a heat source for heat pumps can have positive implications. Daily variation in wastewater temperature is low if compared to environmental air [9], and the average wastewater temperatures are higher than for air in the winter period, meaning that heat pumps should operate more reliably and efficiently. Studies have shown that wastewater heat pumps have already been imple-

* Corresponding author.
E-mail address: angel.a.pardinas@sintef.no (Á.Á. Pardiñas).

https://doi.org/10.1016/j.enbuild.2023.113047
0378-7788/

Nomenclature

A	heat transfer area, m^2
COP	coefficient of performance, –
c_p	specific heat capacity (isobaric), J kg^{-1} K^{-1}
DHW	domestic hot water
DPT	differential pressure transducer
EVAP	evaporator
F	LMTD correction, –
FEM	full-ejector mode
GM	gravity mode
h	specific enthalpy, J kg^{-1}
HFC	hydrofluorocarbon
HFO	hydrofluoroolefin
HP	high pressure
HW	hot water
IHX	internal heat exchanger
LMTD	logarithmic mean temperature difference
LP	low pressure
$\dot{m}$	mass flow rate, kg s^{-1}
MF	mass flow meter
p	pressure, Pa
PID	proportional integral derivative controller
P&ID	piping and instrumentation diagram
PT	pressure transducer
$\dot{Q}$	heat flow rate, W
SH	superheating degree, K
T	temperature, K, °C
TT	temperature transducer
U	overall heat transfer coefficient, W m^{-2} K^{-1}
V	valve
x	vapour quality, –
Δp	pressure drop/lift, bar
ΔT	temperature difference, K
η	efficiency, –

Subscripts

comp	compressor
disch	discharge
ejec	ejector
evap	evaporator
GC	gas cooler
global	global
in	inlet
is	isentropic process
GW	greywater
LMTD	logarithmic mean temperature difference
mot	motive
out	outlet
ref	refrigerant
suc	suction
water	water

mented to some extent [10] and show notable energy savings over air-to-water heat pumps [11].

There have been several works in the literature focusing on heat pumps with wastewater as heat source [12–17] but all considered R134a as the refrigerant. R134a is no longer an option due to the environmental policies looking into phasing out hydrofluorocarbons (HFCs) and, potentially, hydrofluoroolefins (HFOs) in a near future [18,19]. To the best of our knowledge there is only one study that has performed a preliminary analysis on R744 (carbon dioxide, CO_2) heat pump layouts that could use greywater as heat source [20]. R744 is a natural refrigerant with very special thermodynamic properties when utilized in heat pumps, since it operates in transcritical mode due to its relatively low critical temperature (critical point at 30.98 °C and 73.77 bar [21]). The gliding temperature of the gas cooling process can match very tightly the process of DHW production. The increasing importance of DHW production among the thermal loads in buildings combined with stricter environmental legislations are expected to drive a strong market penetration of R744 DHW heat pumps in the coming years [22]. The benefits would be even higher if the greywater resulting from this DHW use were utilized back as heat source for the heat pump.

Moreover, greywater thermal storage may be a key to operate heat pumps relying on greywater as heat source, decoupling DHW consumption from production. To minimize the storage size, the heat in the stored greywater should be utilized down to the lowest possible temperature, but the clear consequence of this would be the reduction in evaporation temperature and heat pump performance. As a solution, a novel, ejector-supported, two-stage evaporator is suggested for this application. Ejector is a well-known technology that has shown its positive impact on CO_2 refrigeration systems and heat pumps [23]. In this case, the ejector would allow dividing the evaporation process in two-stages: the first at higher evaporation temperature and making use of the greywater stream at the inlet (at warmer conditions), and the second at the lowest pressure level in the heat pump and retrieving heat from the greywater stream after the first stage (at colder conditions).

Recently, Cao and co-workers [24] investigated numerically the performance of a vapour compression system with ejector-supported two-stage evaporator, and compared it among others to the basic case of two-stage evaporation in which a compressor handles each suction-pressure level. They demonstrated that implementing the ejector improved the performance compared to having two compressors. Concerning the comparison with a basic ejector cycle, the ejector-supported two-stage evaporator system would be suitable as long as the temperature glide in the heat source would not approach 0 K. Cao et al. pointed out the need for further experimental work on the topic to attain better understanding of the technology.

A relatively similar concept had already been suggested and theoretically investigated by Bai et al. [25], even if in this case it relied on two ejectors and a more complex layout. COP improvements above 30 % were achieved compared to a system relying on one compressor for both evaporator levels. Implementation of the two-stage evaporator concept in heat pumps/chillers for hotel applications was also investigated numerically and in the field [26,27]. The authors show preliminary results and validation of numerical models, but further data would be needed for a more in-depth analysis. Zheng and Deng [28], analysed experimentally a similar system layout, with a variable geometry ejector. Thus, they evaluated how the ejector opening degree, among other parameters, affected the performance of the system in terms of COP and distribution of load between the evaporator stages, but they did not compare the results against a reference scenario.

This article presents the experimental results of the implementation of a novel two-stage evaporator in R744 heat pumps for DHW generation using greywater as a heat source. The novelties of the heat exchanger in this study are that: i) both heat exchanger

stages (brazed plate heat exchangers) were built-up together in the same unit, making it a very compact design, attractive for heat pump manufacturers; and ii) the evaporator is suggested for greywater utilization with large ΔT. The novel evaporator was tested and analysed under various layouts (including two ejector designs) for hydraulic and thermal performance. Moreover, two conventional (one-stage) evaporators were experimentally evaluated for comparison and benchmarking of the novel two-stage configuration. All these results were used with the objective of understanding the potential influence of evaporator selection and ejector implementation on the efficiency/COP of a R744 heat pump. Due to being the first effort in this line, clean tap water was utilized as the heat source in the experimental campaign, disregarding any long-term effect that could be caused by the biofouling on the heat exchanger.

2. R744 heat pump configurations with greywater as heat source

Heat pumps are vapour compression systems with the purpose of transferring heat to a heat sink, from a heat source, elevating its temperature by means of a work input. Heat pumps have in common that they need, at least, four basic components (compressor, two heat exchangers and a throttling device) and a refrigerant circulating through them following the vapour compression cycle. The peculiarity of R744 compared to other refrigerants is its relatively low critical temperature (critical point at 30.98 °C and 73.77 bar), meaning that in heat pump applications the system is operated in transcritical mode. Thus, the heat rejection process occurs at supercritical pressure, with a gliding-temperature gas cooling process instead of condensation, which makes R744 heat pumps suited for hot water production up to temperatures around 90 °C [29]. Fig. 1a represents a basic R744 heat pump, which is equivalent to that introduced by Prof. Gustav Lorentzen [30], with the difference that in this particular case evaporator and suction accumulator are combined. The four basic components mentioned above are: compressor (COMP) to circulate and elevate the pressure of the refrigerant; first heat exchanger (GAS COOLER) to transfer heat to the heat sink, in this case a hot water (HW) loop; throttling device (high-pressure valve HPV) to adjust accordingly the high pressure in the system while expanding the refrigerant to a tank (RECEIVER/EVAP) where the evaporator coil is submerged and retrieves heat from a source. In addition, there is an internal heat exchanger (IHX) to guarantee that the refrigerant stream sucked by the compressor is superheated while the high-pressure stream from the gas cooler is further cooled.

The maximum efficiency of R744 heat pumps is achieved when the return temperature of the heat sink (HW_{in}) is relatively low, e.g., in locations with cold tap water or well-designed systems that accommodate the HW flow rate to minimize the return temperature. However, the exergy losses increase importantly as the gas cooler outlet temperature increases, and thus there is a higher potential of enhancing the heat pump performance (coefficient of performance, COP) through devices that approximate to an isentropic expansion (e.g., expander) rather than to an isenthalpic (such as expansion valves or capillary tubes) [31,32]. An ejector in a heat pump is a device that utilizes the expansion work recovered from the high-pressure stream to circulate a low-pressure stream and elevate its pressure [33]. As shown in Fig. 1b, the high-pressure stream from the gas cooler (and IHX) is the primary flow to the ejector and sucks the refrigerant from the evaporator and compresses it to the receiver pressure, decreasing the compressor pressure ratio and consumption at equal heat source conditions, and increasing the COP in values that range between 7 % and 10 % [34–36].

As already introduced, using greywater as a heat source could further enhance the efficiency of a heat pump, especially if heat transfer occurred directly, without intermediate loops. Mazhar

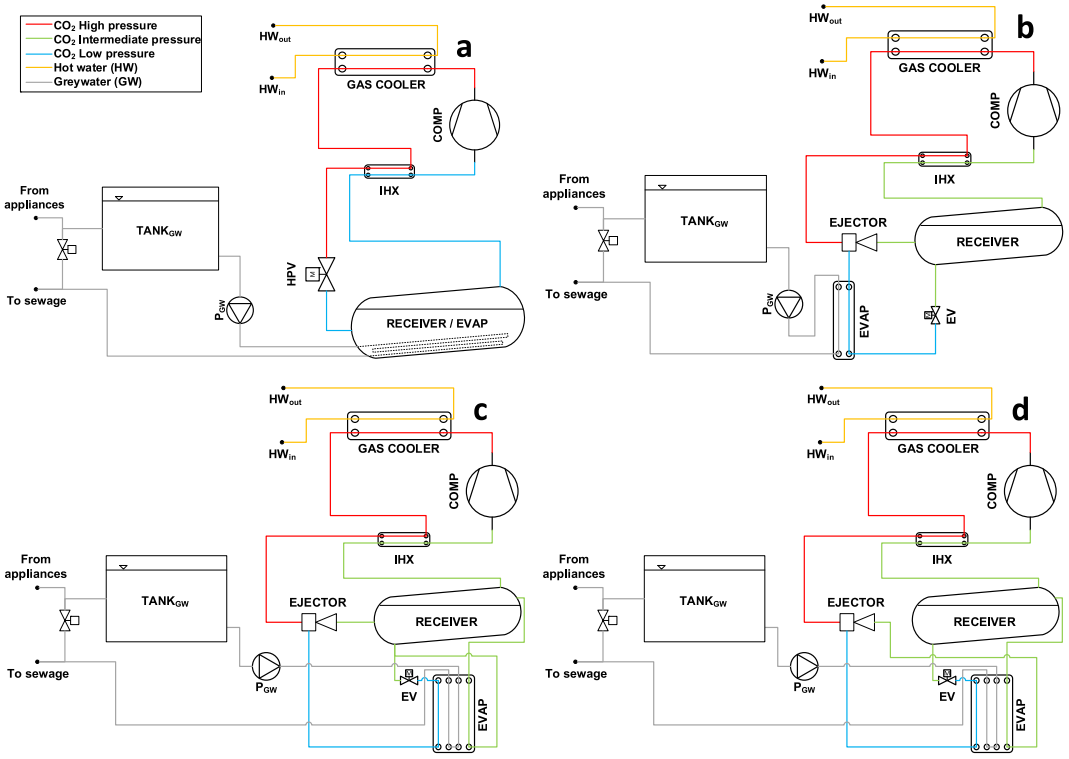

Fig. 1. Suggested R744 heat pump layouts using greywater as heat source. a) With evaporator submerged in the R744 receiver; b) with ejector-supported brazed plate evaporator; with the ejector-supported two-stage evaporator connected in c) gravity-driven mode (GM) or d) full-ejector mode (FEM).

et al. [6] listed the concerns that need to be addressed or considered when harnessing heat from greywater. Storage of the greywater for its use as heat source can tackle several of the challenges, such as the intermittence of availability of the grey water and to decouple it from hot water production. However, space for this storage can be a limiting factor, and the stored greywater would need to be utilized to its maximum potential to minimize the volume of the storage, i.e., a high ΔT needs to be taken from the greywater before it is delivered to the sewage, potentially as low as the freezing temperature of water (plus some Kelvin as safety margin). However, according to Wallin and Claesson [13], there might be some limitations on how low temperature the greywater can reach before drained to the sewage (e.g. never below incoming tap water temperatures). Other factors such as filtration of the greywater and maintenance/rinsing, separation of greywater and blackwater streams or impact of biofouling on the heat pump COP [14] are not addressed in this experimental study, and thus will not be commented further.

The key objective of this study is maximizing the utilization of heat available in stored greywater. As written above, adjusting the greywater flow such that a large ΔT occurs in the evaporator between inlet and outlet is crucial to minimize storage volume, but it also involves that the heat pump evaporation temperature is reduced importantly (obviously below the lowest allowed greywater temperature). This has a negative effect on the heat pump performance which could cancel out the benefits due to utilizing a heat source with relatively high temperature, i.e., greywater if compared with air source in relatively cold climates. Thus, the idea of splitting the evaporation process in two stages while elevating the compressor suction pressure by using an ejector was suggested. This concept was already evaluated and even patented utilizing two evaporators for cabin cooling [37,38] or with separate plate heat exchangers for chillers and heat pumps [26,27,39]. The novelties of the heat exchanger in this study are that: i) both heat exchanger stages (brazed plate heat exchangers) were built-up together, in the same unit; and ii) the evaporator is suggested for greywater utilization with large ΔT. The purpose would be to utilize this heat exchanger in compact units, where it is a clear advantage that water piping between stages is integrated in the heat exchanger. The prototype supplied by Alfa Laval is represented in Fig. 2, indicating the different streams and how they would flow through. The green lines represent the R744-stream through the first stage of evaporation (at highest evaporation temperature). The blue lines correspond to the R744-stream through the second stage of evaporation (at lowest evaporation temperature). The grey lines depict the greywater stream, flowing through the first stage of evaporation (from top to bottom) and then through the second stage of evaporation (from bottom to top), with a pocket in between stages to measure the temperature at that point. A preliminary analysis was performed using this same prototype as evaporator for chillers [40,41]. More details about this prototype are given in Section 3.1.

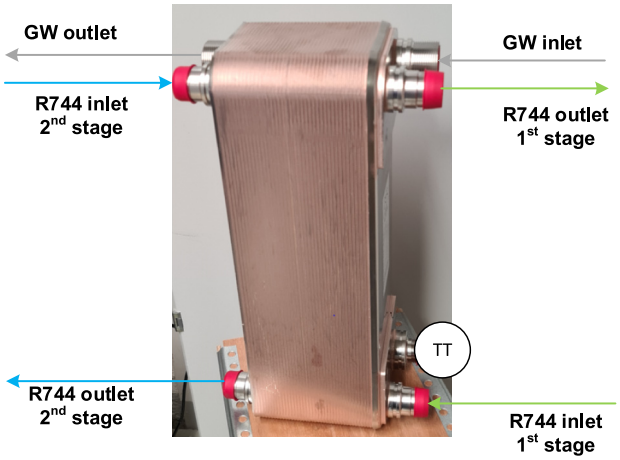

Fig. 2. Picture of the novel two-stage evaporator (uninsulated) with indications about the different streams.

The two-stage evaporator can be implemented in two different ways into a CO_2 heat pump: gravity-driven mode (Fig. 1c) and full-ejector mode (Fig. 1d). In the former, the first stage of the evaporator would be connected to the bottom of the RECEIVER in such a way that the liquid refrigerant is fed to the first stage due to the thermosyphon principle. In the latter, the first stage would receive the refrigerant stream discharged by the ejector. The operation of the second stage of the evaporator would be equivalent in both modes, i.e., with the liquid refrigerant from the RECEIVER expanding through the evaporator expansion valve (EV), and the vapour produced would be sucked by the EJECTOR and lifted back to the RECEIVER pressure. Both options were experimentally tested at equivalent conditions and the comparison is presented in another section. On paper, the full-ejector mode (Fig. 1d) could suffer from refrigerant maldistribution and high pressure drop at the first-stage evaporator due to two-phase flow with relatively high quality at the inlet. On the other hand, this layout should lead to more compact heat pumps as it is possible to avoid the liquid head needed for an efficient operation of the gravity-driven mode (Fig. 1c).

It is worth pointing out that in any of the R744 heat pump layouts shown above, the design of the suction accumulator/receiver and its inlets and outlets is key to avoid droplet carryover to the compressor and securing lubricant recovery, even in units with oil separation downstream of the compressor. As already mentioned by Lorentzen in [30] and very clearly shown in Mineto et al. [32], PAG oils are very well suited for R744 systems with receivers/suction accumulators, due to the differentiation of phases that occurs inside these pressure vessels: oil-rich phase at the bottom, followed by the liquid refrigerant-rich phase and then refrigerant vapour on top. Thus, oil can be returned to the compressor from the very bottom layer of the tank, while liquid refrigerant is fed to the evaporator from a slightly higher port and vapour is sucked by the compressor from the very top of the tank.

3. Experimental methodology

3.1. Heat exchangers tested

The two-stage evaporator prototype tested in this study combines two identical brazed plate heat exchangers type AXP 82 [42] assembled back to back and with a thicker intermediate plate, and with the secondary loops connected internally. Each of these brazed plate heat exchangers had 40 plates, as suggested by the manufacturer to obtain a dimensioning cooling capacity of 40 kW in chiller mode. This number of plates is higher than the 30 plates of the one-stage brazed plate evaporator used as benchmark, being the reason to accommodate the 33 % higher water mass flow rate needed for the 40-kW evaporator if compared to the 30 kW evaporator while avoiding excessive pressure drop. Some of the characteristics claimed by the manufacturer [42] which are important for application in R744 heat pumps with greywater as heat source, are i) high resistance to corrosion, ii) design for high pressures, suited for CO_2 systems, iii) self-cleaning and low level of service or maintenance. In this first iteration, the evaporator was tested without add-on distributor, even if it is offered as an option for these heat exchangers when used as evaporators. The reason that explains this decision was that pressure drop mini-

mization was seen as key, particularly in the first stage of evaporation (higher evaporation temperature), both in gravity-driven mode or when refrigerant was supplied directly from the ejector discharge port. Some of the geometric parameters of the heat exchanger are included in Table 1.

The heat exchangers used as benchmark were two units sized as evaporators for R744 heat pumps with greywater as heat source, but for lower cooling capacity (in this case 30 kW). The first was a one-stage brazed plate evaporator, and the second a shell-and-tube receiver evaporator with R744 forming a pool in the shell and used as receiver/suction accumulator, while greywater circulates through the tube (no parallel circuits) and transfers heat to the R744. Some important details about these two heat exchangers are included in Table 1 (pictures in Appendix A).

3.2. Experimental setup

The heat exchangers above were tested utilizing an experimental setup named MultiTest-Rack (https://www.sintef.no/globalassets/project/highefflab/onepager_multitest.pdf), available in SINTEF/NTNU Varmeteknisk laboratory in Trondheim (Norway). It is a flexible compressor rack (R744 booster system with parallel compression) connected to the components to be tested and to controlled secondary loops to set the operating conditions. A simplified P&ID of the experimental setup is presented in Fig. 3 (and pictures in Appendix A), focusing on the section where the heat exchangers were connected. The compressor rack (compressors, gas coolers, auxiliary heat exchangers and components, etc.) was not represented for simplicity and clarity, and thus the R744 was depicted as an ingoing R744 stream from the gas coolers at high pressure and an outgoing R744 stream at intermediate pressure to the compressors. However, a complete (but still simplified) P&ID and clarification of the whole experimental setup was included in Appendix A.

Table 1
Main parameters of the tested heat exchangers.

	Brazed plate, two-stage evaporator	Brazed plate, one-stage evaporator	Shell-and-tube receiver/ evaporator
Dimensioning capacity [kW]	40	30	30
Total Height [mm]	496	377	–
Useful Height [mm]	415 (410–420)	320	–
Width [mm]	166	119.5	–
Plates [–]	40 + 40	30	–
Hold-up volume [L/channel]	0.095	0.061	–
Estimated average gap [mm/ channel]	1.15	1.35	–
Distributor	NO	NO	–
Volume receiver, shell-side R744 [L]	–	–	210
Tube outer diameter [mm]	–	–	16
Tube inner diameter [mm]	–	–	12
Tube length [m]	–	–	24
Estimation heat exchange source [m^2]	2.6 + 2.6	1.1	1.2
Material heat exchange surface	Stainless steel	Stainless steel	Copper

The different heat exchangers tested can be linked to the operation modes that had been introduced in Fig. 1 as follows:

- Shell-and-tube receiver/evaporator (REC/EVAP in Fig. 3). This heat exchanger is mainly associated with the R744 heat pump layout shown in Fig. 1a.
  - On the R744 side, the main requirements were i) to maintain a sufficient pool of refrigerant in the receiver to submerge the tube surface, and ii) to regulate the pressure at the receiver (measured with PT_2) by adjusting the compressor capacity. The control of the high pressure was in this case not as relevant as when the ejector was employed (see following operating modes) but was kept above the critical pressure for all tests by adjusting the ejector capacity. More information about the ejector(s) used is included below. The reader should be aware that in this case the suction stream to the ejector was totally closed, implying that the ejector was functioning as a high-pressure valve.
  - On the water side, V_{11} was set to the position connecting to the receiver/evaporator tube, V_{13} open and V_{12} closed. The water inlet temperature (measured with TT_{12}) and mass flow rate (registered with MF_{GW}) were adjusted for each test utilizing an electric heater and pump with metering valve downstream, respectively. These components were not represented for clarity.
- One-stage brazed plate bottom-fed evaporator ($EVAP_{1\text{-stage}}$ in Fig. 3). This heat exchanger is associated with R744 heat pumps with a conventional ejector-supported layout, as in Fig. 1b.
  - On the R744 side, three operating conditions were relevant in these tests. First, the ejector motive port temperature (TT_1) and pressure (PT_1), which were adjusted by the control of the ejector capacity and of the heat rejection at the gas cooler (not represented in Fig. 3). Second, the refrigerant mass flow rate through the evaporator ($MF_{ev,2}$), which was a consequence of an open position of V_5 and the control of the expansion valve (V_{evap}) opening degree according to superheating degree at the evaporator outlet, determined by the measurements in TT_4 and PT_4. Third, the evaporation pressure (measured with PT_4), which was indirectly regulated by the effect of the compressor capacity on PT_2 and being the difference between these two pressure transducers the ejector pressure lift.
  - On the water side, V_{11} was set to the position connecting to the brazed plate heat exchangers (V_{12} closed, V_{13} open). The water inlet temperature (measured with TT_{10}) and mass flow rate (registered with MF_{GW}) were adjusted as in the previous case.
- Two-stage brazed plate evaporator ($EVAP_{2\text{-stage}}$ in Fig. 3). This heat exchanger is associated with the R744 heat pumps shown in Fig. 1c and d.
  - The R744 side, second stage, was in essence as the one-stage brazed plated evaporator introduced above, with the main differences that V_4 was opened (and V_5 closed) and that it was top fed with refrigerant to achieve countercurrent streams (R744 and water).
  - For the R744 side first stage, two options were evaluated (in both cases bottom-fed):
    - Gravity-driven mode (Fig. 1c), with the R744 mass flow rate dictated by the relative height between the evaporator and the receiver (and the filling level), the pressure losses and heads in the different lines, and the conditions in the secondary loop (temperature, flow rate). The height of the downcomer in this case was approximately 0.8 m. Even if it was not fully optimized, it had been selected based on a

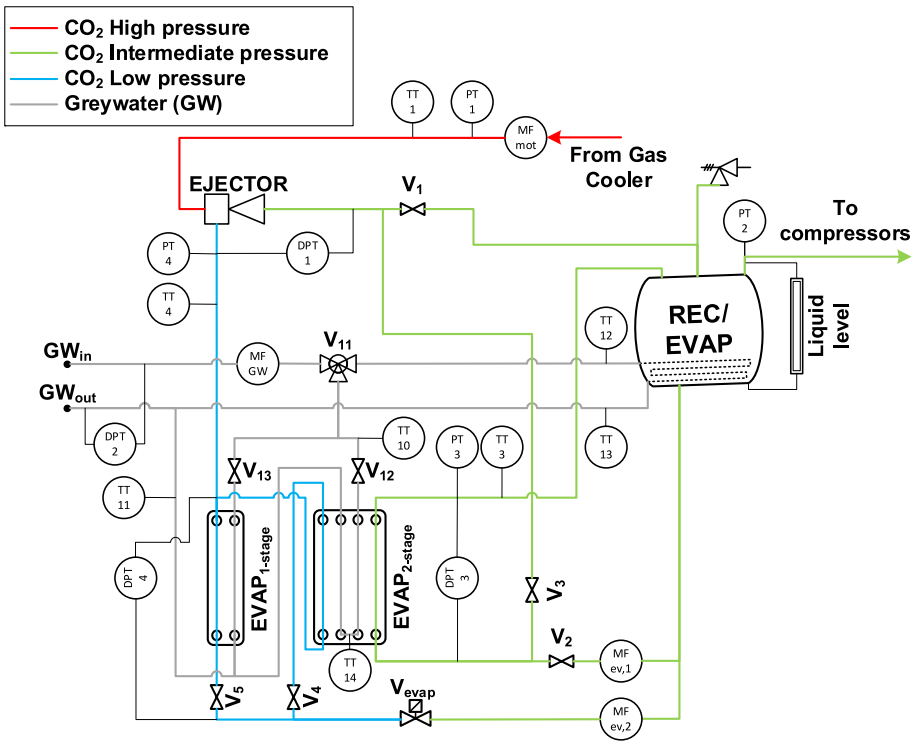

Fig. 3. Sketch of the experimental setup utilized to test the heat exchangers.

preliminary calculation. More data about the gravity-driven loop are included in Appendix A. For this mode, V_1 and V_2 were open and V_3 closed.

- Full-ejector mode (Fig. 1d), with all the flow from the ejector (motive and suction streams) through that evaporator stage. To achieve this, V_1 and V_2 were closed and V_3 open.

  - The water side operation and control is basically the same as in the one-stage brazed plate evaporator, with the particularity that V_{12} is now open and V_{13} closed.

Three out of the four operation modes described above rely on the ejector to function, and thus the ejectors utilized in this article are described in the following. Of the several alternatives to control flow and capacity with ejectors [43], the selected solution was fixed-geometry ejectors arranged in parallel, which has proven successful in the past. The particularity of this flow control approach is that the ejector performance is not so penalised under part load, since there is always an ejector combination to handle the motive flow. As a compromise, the high-pressure control is not as precise, but typically within 1 bar from the setpoint.

The Multi Ejector is a commercial product that operates according to the principle of fixed-geometry ejectors in parallel [44]. Two commercial models were selected for this experimental campaign: the low pressure lift Multi Ejector LP 1935 (six cartridges) and the high pressure lift Multi Ejector HP 2875 (five cartridges). The Multi Ejector LP (LP ejector) would be particularly suited for the system layout with the one-stage evaporator, due to the need for a relatively high entrainment ratio that can be matched by this ejector, and was also evaluated for a R744 heat pump with the two-stage evaporator prototype. However, the high ΔT expected in the greywater side suggested that a HP ejector could lead to even higher compressor suction pressures and heat pump COPs, and thus it was also tested in this study.

The data acquisition system was based on National Instruments hardware and LabVIEW software (sampling rate of 1 s), retrieving data from very precise measurement equipment located as shown in Fig. 3 and with the features listed in Table 2. PIDs were also programmed in the same platform to regulate some of the operating conditions, e.g., greywater temperature, ejector motive temperature and pressure. Other parameters were adjusted with the compressor rack regulator either automatically (evaporator pressure) or manually (greywater mass flow rate).

3.3. Experimental conditions

The experimental conditions considered in this study were as depicted in Table 3, and these values are justified in the following bullet points.

Table 2
List of measurement equipment and accuracy.

Type	Manufacturer and model	Accuracy
Coriolis mass flow meters (MF)	Rheonik RHM[a]	±0.2 % of reading
Pressure transducers (PT)	Endress + Hausser PMP71	±0.075 % of set span[b]
Differential pressure transducers (DPT)	Endress + Hausser PMD75	±0.035 % of set span[c]
Temperature sensors (TT)	Pt 1000 Class A (in flow)	± (0.15 K + 0.002*T[d])

a. $MF_{ev,1}$ → RHM06 // $MF_{ev,2}$ → RHM06 // MF_{mot} → RHM08 // MF_{GW} → RHM08.
b. $PT_1 \in [51,121]$ bar // $PT_2 \in [21,71]$ bar // $PT_3 \in [11,71]$ bar // $PT_4 \in [11,71]$ bar.
c. $DPT_1 \in [0,16]$ bar // $DPT_2 \in [0,5]$ bar // $DPT_3 \in [0,5]$ bar // $DPT_4 \in [0,5]$ bar.
d. T is the temperature measured in °C.

Table 3
Test conditions. In bold, reference values.

Parameter	Range
$T_{GW,in}$ [°C]	**30** / 25 / 20
$\dot{m}_{GW}$ [kg·s^{-1}]	**0.41** ($EVAP_{2\text{-stage}}$) or **0.31** (REC/EVAP and $EVAP_{1\text{-stage}}$)
p_{evap} [bar]	35 / **38** / 41
T_{mot} [°C] / p_{mot} [bar]	**35 / 90**
SH_{evap} [K]	**5**

- Greywater (heat source) inlet temperature ($T_{GW,in}$). These temperature levels were selected according to references such as [6,12,45], and should be more than feasible with separation of wastewater sources and insulated storage.
- Greywater mass flow rate ($\dot{m}_{GW}$). Two different levels were set depending on the heat exchanger considered and on the dimensioning cooling capacity, and assuming a maximum temperature reduction of the water (ΔT_{GW}) in the evaporator of 23 K. For the two-stage evaporator, sized for 40 kW cooling capacity, 0.41 kg·s^{-1} was the value, while for the tank or one-stage evaporator, sized for 30 kW cooling capacity, it was 0.31 kg·s^{-1}.
- Evaporator pressure (p_{evap}). In the case of the brazed plate heat exchangers (one-stage and two-stage evaporators) the value indicated in the table was the setpoint for the lowest pressure in the system, as measured by PT_4. For the receiver / evaporator, the pressure transducer to be considered was PT_2.
- Ejector motive conditions (T_{mot} / p_{mot}). The conditions at the ejector motive port are linked to the heat pump needs/demands, provided that the IHX is properly dimensioned for a subcooling of just a few Kelvin. The R744 gas cooler outlet temperature will depend on the temperature at which the water in the hot water loops is returning, which will be related to the application, i.e., space heating and/or DHW. Many different motive port temperatures and pressures could be selected depending on the demand, system design (DHW production with direct or indirect loop, type of hydronic distribution system) or even location (tap water temperatures vary depending on location and time of the year). All this considered and according to the experience of industrial partners, typical gas cooler outlet conditions would be between 35 °C and 40 °C, and thus the setpoint was set to 35 °C. Correspondingly, the motive pressure was adjusted to 90 bar. The $EVAP_{1\text{-stage}}$ was also tested at 40 °C–100 bar motive nozzle conditions, with minimal implications on the evaporator performance. The results are shown in Appendix B.
- Superheating degree at the ejector-supported evaporator or evaporator stage (SH_{evap}). For this experimental evaluation, the mass flow rate through the one-stage evaporator or through the second stage of the two-stage evaporator, i.e. the mass flow rate sucked/entrained by the ejector, was controlled by the expansion valve V_{evap} to attain a superheating degree around 5 K. This parameter did not apply to the receiver /evaporator tests.

4. Data analysis

For each test condition, data were collected during a minimum of 10 min at steady state conditions, and they were averaged during that period and analysed as described in this section.

The heat flow rate, Q, at the different heat exchangers tested were calculated for both the refrigerant (R744) side and the water side for validation purposes, following Eq. (1) and Eq. (2), respectively. Table 4 summarises the inputs for Eq. (1) and Eq. (2) and shows how each parameter was measured or determined for each heat exchanger. CoolProp [21] was employed to obtain the thermodynamic properties of refrigerants and water throughout this study.

$$\dot{Q}_{ref} = \dot{m}_{ref} \cdot \left(h_{ref,out} - h_{ref,in}\right) \quad (1)$$

$$\dot{Q}_{water} = \dot{m}_{water} \cdot c_{p\,water} \cdot \left(T_{water,in} - T_{water,out}\right) \quad (2)$$

For validation of the experimental setup and data acquisition, the heat flow rates calculated in the CO_2 side (Eq. (1)) and in the water side (Eq. (2)) were compared in parity plots as shown in Fig. 4. Fig. 4a shows the results with the heat exchangers used as benchmarking, i.e., receiver-evaporator (REC/EVAP) and one-stage brazed plate heat exchanger ($EVAP_{1\text{-stage}}$). The validation was satisfactory, as represented in the graph, meaning that the water side calculations (Eq. (2)) could be always utilized to determine the heat flow rate in the evaporator. This was preferred to avoid miscalculations from the CO_2 side (Eq. (1)) due to incomplete evaporation in case it happened in any test.

An equivalent validation was performed with the two-stage brazed plate heat exchanger (Fig. 4b) with specific tests where only one of the stages was active, i.e., CO_2 flowing only through one of the stages but water circulating through both due to the characteristics of the prototype. If stage 1 active, the tests showed that the water flow rate started at a certain temperature, TT_{10}, then cooled down as shown by TT_{11}, and then heated noticeably in the inactive part of the heat exchanger (registered by TT_{14}). The temperature difference determined between TT_{11} and TT_{14} was in the order of +0.5 K to +1 K depending on the test. These values are well above the difference between these two sensors in other validation tests performed with "no heat"-conditions, which were actually in the opposite direction, i.e., TT_{11}–$TT_{14} \approx -0.1$ K. The conclusion would be that part of the heat from the water was transferred to the water in the second stage, and the other part to the CO_2 side (first stage). This involved that there was a better matching between the heat flow rates (CO_2 side vs. water side) in case the water temperatures taken for the evaluation were the inlet and outlet temperatures, TT_{10} and TT_{11} ("b" case in Fig. 4), than if taken only the sensors for the first stage, TT_{10} and TT_{14} ("a" case in Fig. 4). However, and interestingly, such issue was not suggested by data if only stage 2 was active. As depicted in Fig. 4b, there was no difference between case "a" (calculation with TT_{14} and TT_{11}) and case "b" (with TT_{10} and TT_{11}) for these tests. The reason for this is unclear, because both water temperature levels and mass flow rates were in the same order of magnitude for Stage 1 tests and Stage 2 tests, which would discard different distributions of the water stream in the different stages. Even with this slight discrepancy, the conclusion from all the validation tests was that the experimental setup was sound.

A relevant indicator of the performance of a heat exchanger is the logarithmic mean temperature difference (LMTD, ΔT_{LMTD}). It is related to the heat flow rate Q as seen in Eq. (3), where U stands for the overall heat transfer coefficient, F for the LMTD correction factor, and A for the heat transfer area. The LMTD can be calculated for an evaporator as described in Eq. (4). With the heat flow rate and LMTD, the overall heat transfer coefficient is obtained as in Eq. (5).

$$\dot{Q} = U \cdot A \cdot F \cdot \Delta T_{LMTD} \quad (3)$$

$$\Delta T_{LMTD} = \frac{\left(T_{water,in} - T_{ref,evap}\right)/\left(T_{water,out} - T_{ref,evap}\right)}{\ln\left(\left(T_{water,in} - T_{ref,evap}\right)/\left(T_{water,out} - T_{ref,evap}\right)\right)} \quad (4)$$

$$U = \dot{Q}/A \cdot \Delta T_{LMTD} \quad (5)$$

F is considered equal to 1 in purely co-current and counter-current heat exchangers, and typically this also applies to heat exchangers used as condensers or evaporators. This last statement

Table 4
Summary of the inputs to the equations in this section and sensors utilized to measure or determine each input for all the heat exchanger tested.

Parameter	$EVAP_{2\text{-stage,HP}}$	$EVAP_{2\text{-stage,LP}}$	$EVAP_{1\text{-stage}}$	REC/EVAP
$\dot{m}_{ref}$	$MF_{ev,1}$	$MF_{ev,2}$	$MF_{ev,2}$	MF_{mot}
$h_{ref,out}$	f(PT_3, TT_3)[a]	f(PT_4, TT_4)[a]	f(PT_4, TT_4)[a]	f(PT_2, x = 1)
$h_{ref,in}$	f(PT_2, x = 0)	f(PT_2, x = 0)	f(PT_2, x = 0)	f(PT_1, TT_1)[b]
$\dot{m}_{water}$	MF_{GW}	MF_{GW}	MF_{GW}	MF_{GW}
c_{pwater}	f(1 bar, avg(TT_{10},TT_{14}))	f(1 bar, avg(TT_{14},TT_{11}))	f(1 bar, avg(TT_{10},TT_{11}))	f(1 bar, avg(TT_{12},TT_{13}))
$T_{water,in}$	TT_{10}	TT_{14}	TT_{10}	TT_{12}
$T_{water,out}$	TT_{14}	TT_{11}	TT_{11}	TT_{13}
$T_{ref,evap}$	f(PT_3, x = 1)	f(PT_4, x = 1)	f(PT_4, x = 1)	f(PT_2, x = 1)
Δp_{evap}	DPT_3	DPT_4	DPT_4	–
Δp_{ejec}	–	DPT_1 // PT_2–PT_4	DPT_1 // PT_2–PT_4	–
ΔT_{evap}	TT_{14} − f(PT_3, x = 1)	TT_{11} − f(PT_4, x = 1)	TT_{11} − f(PT_4, x = 1)	TT_{13} − f(PT_2, x = 1)

a. Or considering saturated vapour (x = 1) in case the evaporator operates wet.
b. Isenthalpic expansion considered in the ejector without sucked/entrained fluid.

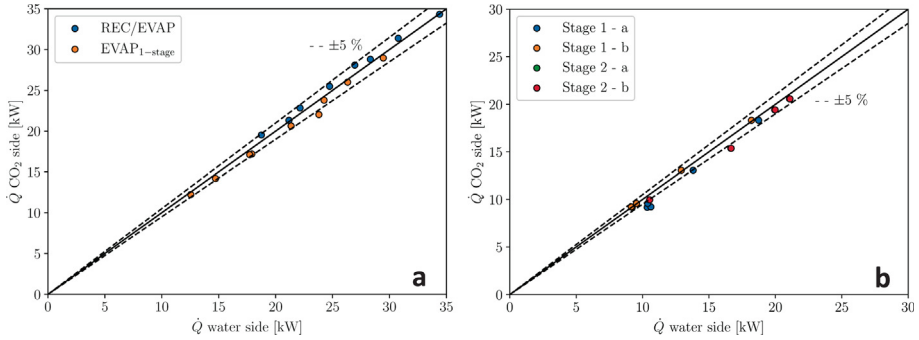

Fig. 4. Parity plots for validation of the experimental setup and data acquisition system, with heat flow rates calculated in the water side (x-axis) vs. those in the CO_2 side (y-axis) for each test condition. a) comparison for the heat exchangers used as benchmark, i.e., evaporator in receiver (REC/EVAP) and one-stage brazed plate evaporator ($EVAP_{1\text{-stage}}$). b) Data from the new prototype of two-stage brazed plate evaporator ($EVAP_{2\text{-stage}}$). In the legend, "a" stands for results calculated from the temperature sensors in the water side corresponding to the active stage in each case, namely TT_{10} and TT_{14} for Stage 1 and TT_{14} and TT_{11} for Stage 2. On the other hand, "b" corresponds to values for which the sensors considered were those at the inlet and outlet of the heat exchanger, i.e., TT_{10} and TT_{11} independently of the stage.

was analysed numerically in reference [46], and it was seen that F would only be below 0.95 in case very low LMTD were achieved (below 3 or 4 K), being safe to consider $F = 1$ for further calculations of the overall heat transfer coefficient U (Eq. (5)). The heat transfer areas from Table 1 were taken in each case.

The main difference between the heat exchangers tested is which sensors were utilized for each evaluation, and this is indicated in Table 4. It is important to specify that constant evaporation temperature and no superheat were assumed in these calculations (refrigerant side). These assumptions could be disputed when observed the results indicated in the corresponding section, particularly for Stage 1 in the two-stage evaporator ($EVAP_{2\text{-stage}}$). On the one hand, the superheating degree of the gravity-driven tests was significant. On the other hand, the pressure drop (CO_2 side) with full-ejector mode tests (ejector discharge through Stage 1) was not negligible, but fortunately CO_2 has a rather low change of saturation temperature with pressure drop [47]. All in all, the evaluation with the abovementioned assumptions was considered sufficiently accurate for this comparison study.

The temperature approach at the outlet of each evaporator, ΔT_{evap}, was also calculated as shown in Eq. (6), corresponding to the difference between the water temperature at the outlet and the evaporation temperature. The sensors used for each evaporator are indicated in Table 4.

$$\Delta T_{evap} = T_{water,out} - T_{ref,evap} \quad (6)$$

Finally, the pressure variations through the heat exchangers (pressure drops) and due to the ejectors (pressure lifts) were analysed. As indicated in Table 4, dedicated differential pressure sensors exist for the brazed plate evaporators ($EVAP_{1\text{-stage}}$ and for each stage of $EVAP_{2\text{-stage}}$). Concerning the ejector pressure lifts, i.e., the potential improvement of compressor suction pressure, two alternative methods for evaluation where compared: i) with the differential pressure sensor at the ejector ports, measuring purely the ejector pressure lift; and ii) as the difference between the receiver pressure transducer and the evaporator pressure transducer, thus covering also any potential pressure drop in the lines and even heat exchangers (such as in the full-ejector mode with the $EVAP_{2\text{-stage}}$).

The Guide for Uncertainty of Measurement [48] was followed for the uncertainty analysis in this study. Uncertainties in the Guide are classified as type A and type B:

- Type A uncertainties. Due to standard deviations of the parameters during the test.
- Type B uncertainties. Based on the sensors and databases utilized to measure and/or determine thermodynamic properties. In the case of sensors, information from the datasheets by the manufacturers was included in Table 2.
  - o Due to the lack of precise information in these datasheets, the worst case was assumed, i.e., sensor accuracy is indicated with a coverage factor equal to 1. However, the Guide [48] was followed when it is suggested that the accuracies indicated can be divided by the square root of three if uniform distribution of the measurements can be assumed.
  - o The thermodynamic properties of R744 and water were obtained from CoolProp [21], and their uncertainties were evaluated as described in reference [49] and based on the uncertainty of each of the parameters used in their determination.

Table 5
Average relative uncertainties (in percentage) of some of the parameters determined during the experimental campaigns, for the different configurations.

Tests	Q_{water}	ΔT_{LMTD-1}	ΔT_{LMTD-2}	$U{\cdot}A_{LMTD-1}$	$U{\cdot}A_{LMTD-2}$	$\Delta p_{ejec,calc}$	$\Delta p_{ejec,DPT}$
REC/EVAP	1.00 %	7.71 %	–	7.78 %	–	–	–
$EVAP_{1\text{-stage}}$	1.23 %	4.40 %	–	4.58 %	–	1.31 %	0.80 %
$EVAP_{2\text{-stage}}$-HP-FEM	1.99 %	20.66 %	4.86 %	20.77 %	5.14 %	1.03 %	0.82 %
$EVAP_{2\text{-stage}}$-HP-GM	1.72 %	3.78 %	4.31 %	5.96 %	5.18 %	1.05 %	0.80 %
$EVAP_{2\text{-stage}}$-LP-FEM	1.41 %	15.18 %	7.98 %	15.22 %	17.31 %	1.35 %	0.58 %
$EVAP_{2\text{-stage}}$-LP-GM	2.73 %	3.33	4.07 %	5.37 %	6.95 %	1.32 %	0.86 %

- The uncertainties of other parameters and indicators which are not directly measured or evaluated were calculated following the propagation of uncertainties methodology as defined in the Guide [48].

Uncertainties were not represented in the figures included in this article for the sake of clarity, but they were summarised in Table 5, in the form of relative uncertainties (considering a coverage factor of 1). It is worth pointing out the relatively high uncertainties for the LMTD in those cases where the temperature approach in the heat exchanger (or stage of the heat exchanger) was very low. A high LTMD uncertainty has a clear impact on the *U·A* uncertainty.

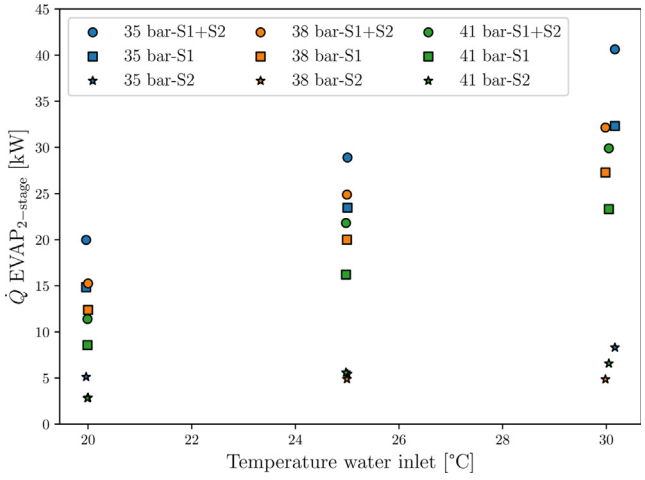

Fig. 5. Heat flow rate at $EVAP_{2\text{-stage}}$ in full-ejector mode and using the HP ejector, as a function of water temperature at the evaporator inlet, and at different evaporation pressures (considered the lowest level at the evaporator). Legend shows the lowest evaporation pressure (at Stage 2) and to which stage or stages each data point corresponds. Circles represent the aggregated heat flow rate of both stages (S1 + S2), squares to Stage 1 (S1) and stars to Stage 2 (S2).

5. Results and discussion

5.1. Evaporator results

Fig. 5 represents the heat flow rate obtained with the two-stage brazed plate evaporator ($EVAP_{2\text{-stage}}$) with HP ejector and operating in full-ejector mode, as a function of water inlet temperature and lowest evaporation pressure (thus at Stage 2). The dimensioning heat flow rate (40 kW) was attained with the lowest evaporation pressure (35 bar) and highest water inlet temperature tested (30 °C). Even if increasing the evaporation pressure had an impact on the heat flow rate at the evaporator, the most important effect came from the water temperature at the evaporator inlet (in the range considered). This proved the great importance of having a proper greywater source at sufficiently high temperature to maximize the heat pump output with higher efficiency.

As also depicted in Fig. 5, there was little participation of Stage 2 in the total heat flow rate, between 10 % and 20 %. This was characteristic of $EVAP_{2\text{-stage}}$ operating with full-ejector mode if compared to gravity mode (later shown in Fig. 6) and independently of the ejector type tested. The reason for this was the relatively low CO_2 mass flow rate that could be expanded by V_{evap} and distributed through Stage 2 due to the condition of superheating degree at the outlet (5 K), involving that it performed relatively poorly, which will be discussed later in this section. It is worth pointing out here that the CO_2 liquid stream to Stage 2 in the conditions represented in Fig. 5 was so low that it was not possible to control the opening of V_{evap} according to the superheating degree at the outlet. Thus, in some cases the expansion valve was adjusted to attain an ejector pressure lift in the range of 5.5 bar and 6 bar.

Fig. 6 compares the heat flow rate for $EVAP_{2\text{-stage}}$ with different ejector designs, namely HP ejector (Fig. 6a) and LP ejector (Fig. 6b), and under the different operation modes, i.e., full-ejector mode or gravity-driven mode. The distribution of load between the different stages was clearly connected to the operation mode of the first stage. As mentioned before, Stage 2 had a very small participation in the total heat flow rate when Stage 1 operated with the stream discharged by the ejector (full-ejector mode). However, Stage 2 had

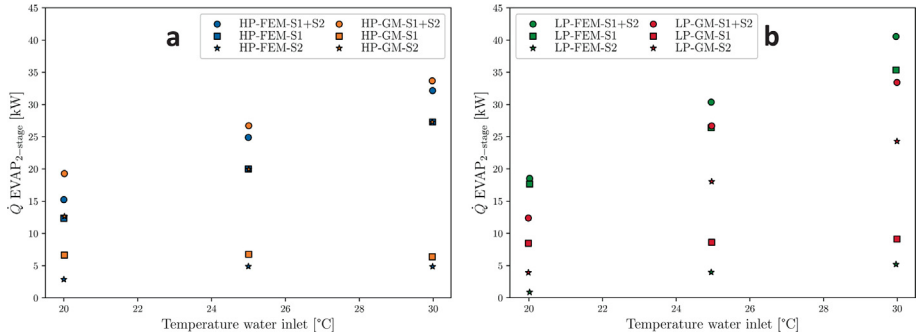

Fig. 6. Heat flow rate at $EVAP_{2\text{-stage}}$ in full-ejector mode (FEM) or gravity-driven mode (GM), as a function of water temperature at the evaporator inlet, and at 38 bar evaporation pressure at Stage 2. a) Tests with high pressure lift (HP) ejector. b) Tests with low pressure lift (LP) ejector. Circles represent the aggregated heat flow rate of both stages (S1 + S2), squares to Stage 1 (S1) and stars to Stage 2 (S2).

a much higher importance when Stage 1 operated in gravity-driven mode. The gravity driven loop in this experimental setup was unable to attain the working conditions that had been estimated during the design phase. The superheating degree at the outlet (CO_2 side) was too high, the reason probably being unaccounted pressure drops in the lines (e.g., mass flow meter at the downcomer) [40]. Thermosyphon loops are very delicate to pressure drop, and this issue will be further investigated by readjusting the vertical distance between receiver and evaporator or removing the mass flow meter. All in all, the relatively low performance of Stage 1 left sufficiently high temperature of the water at the inlet of the Stage 2, and thus the CO_2 stream expanded through V_{evap} could be higher and the evaporator performed much better.

The heat flow rates attained with the LP ejector (Fig. 6b) and the HP ejector (Fig. 6a) were very similar under gravity mode, but they were significantly higher with the LP ejector when $EVAP_{2\text{-stage}}$ was operated under full-ejector mode. This different behaviour can be explained by the fact that the evaporation pressure values at Stage 1 (S1) are very dependent on the ejector type. As represented in Fig. 7a, this pressure was around 4–5 bar lower with the LP ejector, involving that more heat could be retrieved from the water stream, if considered equal water temperature at the inlet. However, it is important to define the effect that the ejector utilized may have on the efficiency of a R744 heat pump, as discussed in Section 5.3.

The pressure drops in Stage 1 and Stage 2 of $EVAP_{2\text{-stage}}$ were measured for each test, but they were only worthwhile in Stage 1. Thus, only the pressure drop for this stage is illustrated in Fig. 7b. When the evaporator was tested in gravity mode, the pressure drop was rather low, even if slightly higher values could be expected with a better performing thermosyphon loop, reaching higher heat flow rates by using higher height at the downcomer. On the other hand, the pressure drop at Stage 1 operated in full-ejector mode was as high as approximately 0.8 bar, the reasons being the high CO_2 mass flow rate, combination of the motive and suction ejector streams, and the vapour quality range in the evaporator, relatively high already at the inlet due to these combined streams. If compared the data as a function of the ejector, the pressure drops were higher with the LP ejector than with the HP ejector. The main cause was that the CO_2 mass flow rates with the LP-ejector tests were slightly higher than with the HP-ejector tests at equivalent water conditions (temperature at the inlet and mass flow rate).

The evaluation of the two-stage evaporator described in this section showed that its performance was completely dependent on the layout utilized (full-ejector mode vs. gravity mode) and on the ejector utilized (HP vs. LP). Stage 1 functioned better with full-ejector mode than with gravity-mode, achieving higher heat flow rate at equivalent conditions at cost of relatively high pressure drop. Even if the thermosyphon loop in Stage 1 could be optimized with the evaporator in gravity mode, it is unclear if this would compensate the benefit that a full-ejector implementation gives in terms of compacity. All this considered, for subsequent sections and comparisons, only the results obtained with full-ejector mode were used.

Optimizing the performance and control of the triad $EVAP_{2\text{-stage}}$, ejector and expansion valve V_{evap} is expected as a challenging task. The distribution of heat flow rate between Stage 1 and Stage 2 is very sensitive to the performance of the ejector (pressure lift and entrainment ratio) as a function of the suction stream conditions (controlled by V_{evap}). The optimization of performance and control strategy is considered out of the scope of this article and will be analysed in future studies.

5.2. Comparison with benchmark heat exchangers

Since this article focuses on the novel two-stage brazed plate evaporator ($EVAP_{2\text{-stage}}$), the raw values of heat flow rate or pressure drop for the benchmark heat exchangers were not specifically

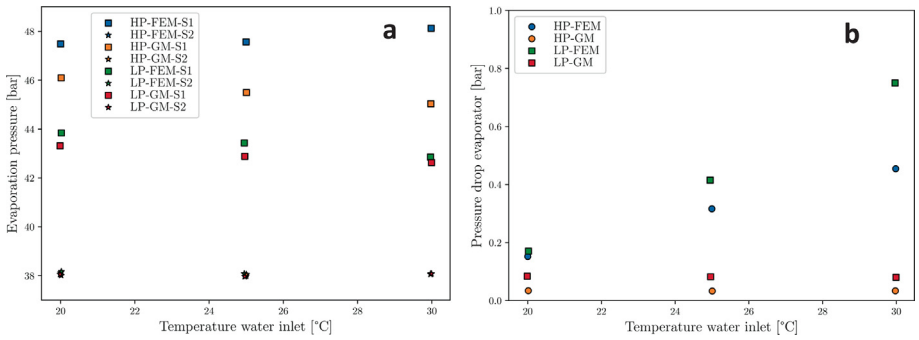

Fig. 7. a) Pressure at the different $evap_{2\text{-stage}}$ stages (S1 and S2) under full-ejector mode (FEM) or gravity-driven mode (GM). Data with high pressure lift (HP) and low pressure lift (LP) ejector are represented. b) Pressure drop at Stage 1. In both cases, results shown as a function of water temperature at the evaporator inlet and 38 bar evaporation pressure at Stage 2.

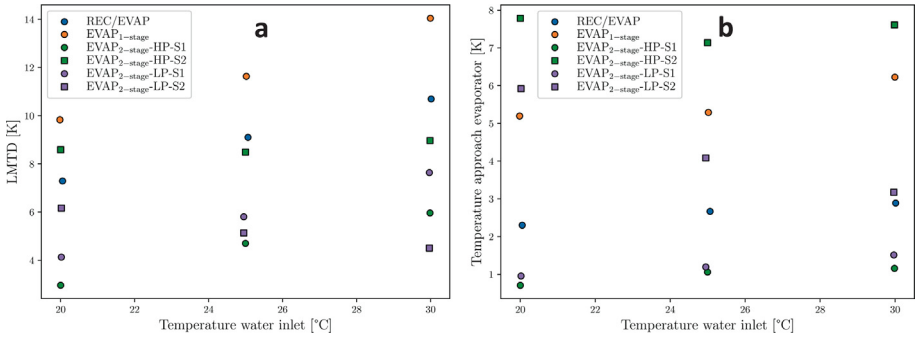

Fig. 8. LMTD (a) and temperature approach at the evaporators (b) as a function of the water temperature at the inlet and at 38 bar evaporation pressure. HP and LP standing for high pressure and low pressure lift ejector, respectively. S1 and S2 representing each of the stages of $EVAP_{2\text{-stage}}$.

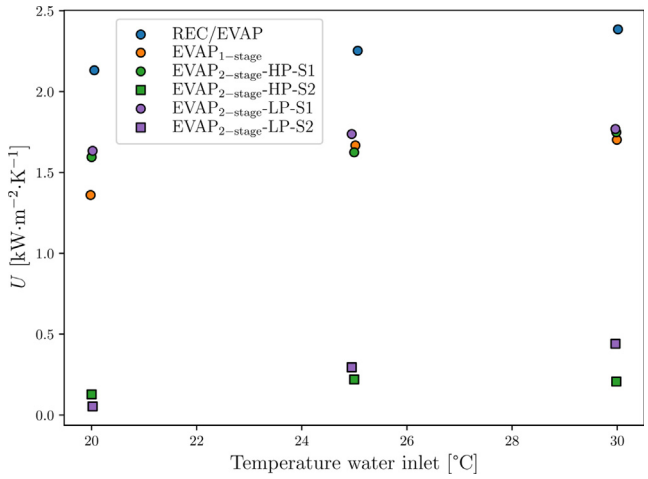

Fig. 9. Overall heat transfer coefficient U as a function of the water temperature at the evaporator inlet for the different heat exchangers tested, at 38 bar evaporator pressure.

shown in the main text. However, they are included in Appendix B for interested readers.

Direct comparison of heat flow rates attained for the heat exchangers was not adequate, as they were sized for different heat flow rates and tested with the water mass flow rate corresponding to their dimensioning. However, the LMTD and temperature approach at the evaporator outlet give a good indication of whether the heat exchanger was dimensioned properly and is suited for the application or not. As shown in Fig. 8a, the LMTD values were lowest in both stages of $EVAP_{2\text{-stage}}$, independently of the ejector utilized, which was related to the fact that splitting the evaporation process in two diminished also the temperature difference at the evaporator inlet, i.e., between the evaporation temperature and the water inlet temperature. From the benchmark evaporators, REC/EVAP had a relatively low LMTD, even if compared with $EVAP_{2\text{-stage}}$, indicating that this evaporator option performed very nicely. This statement is even clearer when considered the temperature approach (Fig. 8b), which corresponds to the difference between the water temperature at the outlet and the evaporation temperature (see Table 4). In the case of the REC/EVAP, it was around 2.5 K in all the tests included in the chart, between half and a third of the value calculated for the one-stage brazed plate evaporator ($EVAP_{1\text{-stage}}$) or for Stage 2 of the two-stage brazed plate evaporator ($EVAP_{2\text{-stage}}$). Only Stage 1 of $EVAP_{2\text{-stage}}$ registered lower temperature approaches than REC/EVAP, in the range of 1 K and independently of the ejector used.

The overall heat transfer coefficients *U* for the different heat exchangers and tests are represented in Fig. 9. In agreement with the findings indicated in the previous paragraph, REC/EVAP led to a rather high *U* compared to the other heat exchangers. It is worth mentioning that the velocity of the water through the pipe in REC/EVAP was large due to the way the evaporator was conceived (see Appendix B) meaning that the water side heat transfer coefficients were most likely higher in REC/EVAP than in the brazed plate heat exchangers ($EVAP_{1\text{-stage}}$ and $EVAP_{2\text{-stage}}$). Moreover, CO_2-side heat transfer coefficients in pool boiling are rather high (easily reaching 20 $kW{\cdot}m^{-2}{\cdot}K^{-1}$ or higher at reduced pressure around 0.5 and with 20 $kW{\cdot}m^{-2}$ heat flux [50]). On the other hand, it must be remembered that the volume of the REC/EVAP, CO_2 charge needed to submerge the whole heat-exchanger surface, etc., could advise against this evaporator, and more if considered that the ejector-supported evaporators are linked to an increase of the R744 heat pump efficiency.

Fig. 9 pinpoints that there is a potential of improving the ejector-supported side (Stage 2) of $EVAP_{2\text{-stage}}$, which was also clear from the temperature approach for Stage 2 and HP ejector in Fig. 8b. Lower heat transfer coefficients could exist in a flow boiling process than in pool boiling, and even more if considered that deterioration at conditions close to dryout [51,52]. Even so, the dominating thermal resistance would not be at the CO_2-side. Considering the low CO_2 mass flow rate through Stage 2 compared to Stage 1, and the fact that this two-stage evaporator prototype was composed of two identical brazed plate heat exchangers, with the same number of plates, refrigerant maldistribution and low velocities could explain the low *U* in Stage 2. Thus, a better heat exchanger construction would probably involve a lower number of plates for the Stage 2 than Stage 1 (keeping in mind pressure drop at the water side). Alternatively, liquid distributors are typically offered by manufacturers to minimize this effect. Refrigerant maldistribution could also be behind the relatively high temperature approach for $EVAP_{1\text{-stage}}$, moreover if compared with the data from the software supplied by the manufacturer, which at equal conditions indicated 2 to 3 K lower temperature approach.

5.3. R744 heat pump performance with the different evaporators

According to the results of the experimental evaluation, it can be concluded that R744 heat pumps could utilize any of the heat exchangers tested. However, the ejector and its pressure lift are expected to increase the heat pump efficiency (COP). In this subsection, a numerical analysis of the potential enhancements due to the implementation of ejector and even two-stage evaporator were performed. The following considerations were taken:

- From the experimental data, it was determined which would be the maximum evaporation pressure that would involve reaching the dimensioning heat flow rate for each evaporator, namely 30 kW for REC/EVAP and $EVAP_{1\text{-stage}}$ and 40 kW for $EVAP_{2\text{-stage}}$ (both HP and LP ejector, in full-ejector mode). These pressures were 38 bar for the REC/EVAP and $EVAP_{2\text{-stage}}$ with LP ejector, and 35 bar for the other two evaporators ($EVAP_{1\text{-stage}}$ or $EVAP_{2\text{-stage}}$ with HP ejector). These values of pressure were obtained with reference greywater conditions, i.e., temperature at the inlet 30 °C and mass flow rate 0.41 or 0.31 $kg{\cdot}s^{-1}$ (depending on the evaporator).

Table 6
Results from the numerical evaluation of R744 heat pumps implementing the different heat exchangers evaluated in this study.

R744 HP with:	REC/EVAP	$EVAP_{1\text{-stage}}$	$EVAP_{2\text{-stage}}$ HP ejector	$EVAP_{2\text{-stage}}$ LP ejector
Evaporation pressure [bar]	38.06	34.98	34.91	38.06
Suction pressure compressor [bar]	38.06	39.33	44.93	42.54
Superheating suction compressor [K]	5			
Discharge pressure compressor [bar]	90			
Gas cooler outlet temperature [°C]	35			
Compressor global efficiency [–]	0.71	0.71	0.70	0.70
COP [–]	3.78	3.87	4.48	4.20
$COP_{enhancement}$ [%]	–	+2.2	+15.5	+10.0

- The receiver pressure in the ejector-supported cases was also taken from the tests. In this manner, it was unnecessary to estimate the ejector efficiency or entrainment ratio.
- The gas cooler pressure and outlet temperature were set at 90 bar and 35 °C, respectively, for this evaluation. Justification for this selection was indicated in Section 3.3.
- The compressor global efficiencies $\eta_{global,comp}$ were evaluated according to Eq. (7) [53]. This efficiency was utilized to obtain the enthalpy at the compressor discharge as in Eq. (8).
- The COP was calculated as indicated in Eq. (9). The COP for a R744 heat pump with REC/EVAP was used as reference to calculate the enhancement due to the alternative ejector-supported evaporators ($EVAP_{1\text{-stage}}$ and $EVAP_{2\text{-stage}}$).
- All thermodynamic properties needed for the analysis were obtained from CoolProp [21].

$$\eta_{global,comp} = -0.0788 \cdot \left(\frac{p_{disch,comp}}{p_{suc,comp}}\right)^2 + 0.3708 \cdot \left(\frac{p_{disch,comp}}{p_{suc,comp}}\right) + 0.2729 \quad (7)$$

$$h_{disch,comp} = h_{suc,comp} + \frac{h_{disch(is),comp} - h_{suc,comp}}{\eta_{global,comp}} \quad (8)$$

$$COP = \frac{h_{disch,comp} - h_{GC,out}}{h_{disch,comp} - h_{suc,comp}} \quad (9)$$

The inputs and results of this evaluation are included in Table 6. Almost all the improvement due to the LP ejector in the case of $EVAP_{1\text{-stage}}$ was compensated by the lower evaporation pressure needed to attain equivalent heat flow rate as with REC/EVAP. Thus, the COP enhancement was just above 2 %, but could be potentially higher with a better designed brazed plate heat exchanger. On the other hand, the enhancement in COP due to the implementation of $EVAP_{2\text{-stage}}$ with ejector was more relevant. The reason for this result is that the heat pump benefits of having the low temperature of Stage 2, utilizing the heat source with an even higher temperature glide, but with a lower suction mass flow rate to be sucked by the ejector than in $EVAP_{1\text{-stage}}$, since part of the heat flow rate already happens in Stage 1. All this while being able to elevate the compressor suction pressure due to the ejector pressure lift (function of the ejector design). The increase in COP was 10 % when the LP ejector was used with that evaporator, as the lowest evaporation pressure was equivalent to that with REC/EVAP, namely 38 bar, while the compressor suction pressure could be elevated by 4.5 bar approximately, to 42.5 bar. Interestingly, with the HP-ejector the pressure needed at Stage 2 of the evaporator was 35 bar due to poor performance of this stage and relatively high evaporation pressure of Stage 1. Even so, it was this R744 heat pump which achieved highest COP, more than 15 % higher than with the REC/EVAP, with a compressor suction pressure of approximately 45 bar. The scenario could be different in case of lower temperature glide in the evaporator secondary fluid, when a HP-ejector would not be utilized fully, and the LP-ejector would lead to higher performance.

6. Conclusions

This article describes the experimental evaluation of a novel, two-stage, ejector-supported, brazed plate evaporator applied in R744 heat pumps for DHW generation using greywater as heat source. The main aim of such evaporator concept is to split the evaporation process in two stages. Thus, greywater utilization is maximized (large temperature glide and reduced flow needed) while keeping or even elevating the compression suction pressure, enhancing the efficiency of such heat pumps. The prototype was built with two conventional brazed plate heat exchangers placed back-to-back and with series connection on the water side, leading to a very compact design, easy to implement by heat pump manufacturers.

The experimental campaign has shown that the side with highest evaporation temperature (Stage 1) can be operated either with a thermosyphon loop (gravity-driven mode) or with a forced flow of the stream discharged by the ejector (full-ejector mode). The full-ejector mode has a very good potential in terms of heat transfer, at cost of non-negligible pressure loss at the CO_2 side. The implementation of the two-stage evaporator in full-ejector mode could be preferred for a compact heat pump design, if compared to a thermosyphon loop, which needs a certain height to perform.

The ejector-supported side of the evaporator (Stage 2) took a much lower share of the load at the tested conditions (Stage 1 operating in full-ejector mode) and independently of the ejector used (high pressure lift or low pressure lift ejector). Even so, Stage 2 underperformed according to the test results, with relatively high temperature approach between CO_2 and water. Future designs and investigations of the two-stage evaporator could: (i) include a lower number of plates in Stage 2 compared to Stage 1; (ii) incorporate a liquid refrigerant distributor at Stage 2 inlet to avoid maldistribution; or (iii) change the evaporator arrangement so that Stage 2 becomes bottom-fed instead of top-fed (while Stage 1 would become co-current). Furthermore, validation tests showed a non-negligible heat transfer between Stage 1 and Stage 2 that will be considered in future iterations of this prototype. The control of the expansion valve that supplies refrigerant to Stage 2 could also be analysed in more detail, since it has an important impact on the performance of the ejector (due to the conditions of the ejector suction stream) and on the share of loads between stages.

The novel two-stage evaporator was compared against two conventional evaporators, a shell-and-tube evaporator and an ejector-supported brazed plate evaporator. The results show that, even if these benchmark heat exchangers can outperform the two-stage evaporator in some cases, with higher evaporation temperature needed for equivalent thermal load at similar conditions, the suction pressure at the compressor ends up being higher due to the ejector. A simplified numerical model of a R744 heat pump indicates that the implementation of two-stage evaporator and low pressure lift ejector improves its COP by 10 % compared to an equivalent heat pump with the shell-and-tube evaporator. This enhancement is above 15 % if the high pressure lift ejector is used instead.

Data availability

Data available in data repository Zenodo at https://doi.org/10.5281/zenodo.7099551.

Declaration of Competing Interest

The authors declare that they have no known competing financial interests or personal relationships that could have appeared to influence the work reported in this paper.

Acknowledgments

The authors would like to acknowledge the great support provided by project ChinoZEN – Key technologies and demonstration of combined cooling, heating and power generation for low-

carbon neighbourhoods/buildings with clean energy (Norwegian Research Council, 304191) to perform the experimental evaluation, analysis of results and preparation of this article. The authors are very grateful also to the company Winns AS, which allowed us to use some of the data registered during the research project HeatJet – Throttling-free, ejector-based CO_2 heat pump (Norwegian Research Council 309314), cofunded by the Research Council of Norway. Last, the authors appreciate the support given by Alfa Laval providing the two-stage evaporator that was core of this article through the project HighEFF – Centre for an Energy Efficient and Competitive Industry for the Future, an 8-years' Research Centre under the FME-scheme (Centre for Environment-friendly Energy Research, 257632).

Appendix A. Experimental system and heat exchangers tested

A picture of the two-stage evaporator tested was already included in Section 2, but will be added here also for completeness (Fig. A.1a). Information about the different distances and heights in the system, relevant particularly for the gravity-driven operation mode (GM), is included in the Table A.1 (based on the schematic in Fig. A.1b).

The first of the evaporators used as benchmark, the one-stage brazed plate evaporator ($EVAP_{1\text{-stage}}$) is shown in Fig. A.2, while the receiver with submerged evaporator (REC/EVAP) is depicted in Fig. A.3.

Two pictures of the experimental setup are included in Fig. A.4, showing the position of two out of the three heat exchangers tested and also the great number of sensors/transducers installed in the unit. In addition, a simplified P&ID is included in Fig. A.5 and consists of the section with the heat exchangers and the main components in the compressor pack used in the experimental setup. Two compressors (COMP) with variable speed drive were used in the compressor rack to control the conditions in the REC/EVAP. Their suction pressures were slightly different, which was adjusted depending on the operating conditions by a valve denoted as flash-gas bypass valve (FGBV). The refrigerant discharged by the compressors flowed through an oil separator, to reduce its oil content, Then, it was cooled down in two steps, first in a brazed plate gas cooler against a glycol stream, and then in another equivalent heat exchanger with a controlled water loop adjusting the conditions at the ejector motive (primary) port. All the high-pressure stream flowed through the ejector, being the high-pressure valve (HPV) fully closed, and just utilized as a safety measure in case of abnormal increase of the pressure. After the ejector, the refrigerant reached the section with the heat exchangers tested, already clarified in Section 3.2. The vapour refrigerant from the REC/EVAP flowed through an oil-return device and to the actual receiver of the compressor rack, from which it was sucked by the compressors.

Table A1
Dimensions of the gravity-fed evaporator loop.

Dimensions		
Height downcomer [m]	H	0.795
Length downcomer [m]	l_{dc}	1.5
Height evaporator [m]	h	0.42
Height riser [m]	H_0	0.63
Length riser [m]	L_{rs}	2.15
Pipe diameter [m]	d_i	0.014

Fig. A2. One-stage brazed plate evaporator used as benchmark ($EVAP_{1\text{-stage}}$).

Fig. A3. Receiver / evaporator used as benchmark (REC/EVAP).

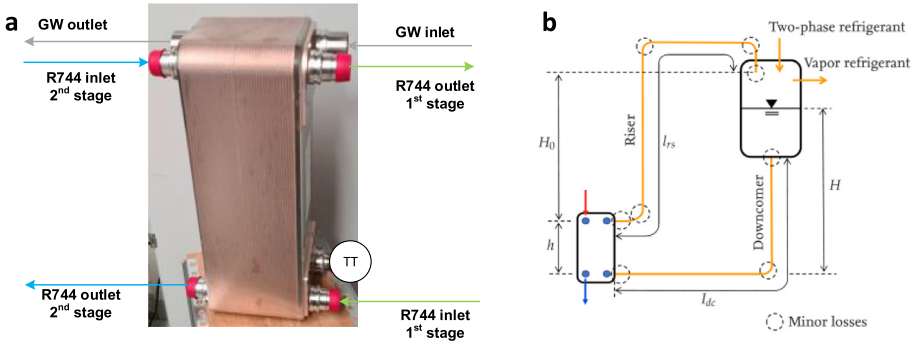

Fig. A1. a) two-stage brazed plate evaporator focus of this article ($EVAP_{2\text{-stage}}$). b) schematic diagram of the gravity-fed evaporator loop (Stage 1 of $EVAP_{2\text{-stage}}$).

Fig. A4. Pictures of the experimental setup.

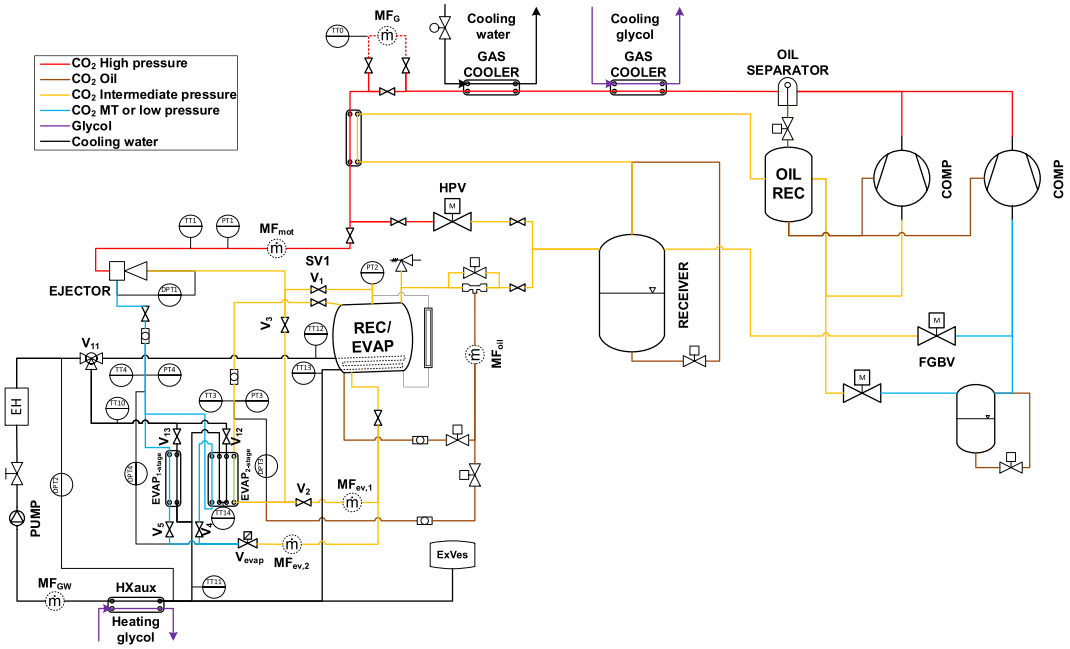

Fig. A5. Simplified P&ID of the complete experimental setup.

Appendix B. Additional results on heat exchangers used as benchmark

This appendix includes results obtained for the heat exchangers used as benchmark in this article.

Fig. B.1 illustrates the experimental results for the one-stage brazed plate evaporator ($EVAP_{1\text{-}stage}$), with the main purpose of showing the effect of ejector motive conditions on the evaporator performance. With the motive nozzle conditions considered, there was negligible impact of this parameter on the evaporator heat flow rate. However, the ejector operated differently as observed with the mass entrainment ratio (ratio of entrained mass flow rate to motive mass flow rate, Fig. B.1), or the pressure lift (difference between pressures at ejector discharge and suction ports, Fig. B.1b). The ejector efficiency (Fig. B.1d) defined as in reference [35].

The specific data for the receiver with evaporator submerged (REC/EVAP) are indicated in Fig. B.2. It is worth pointing out that

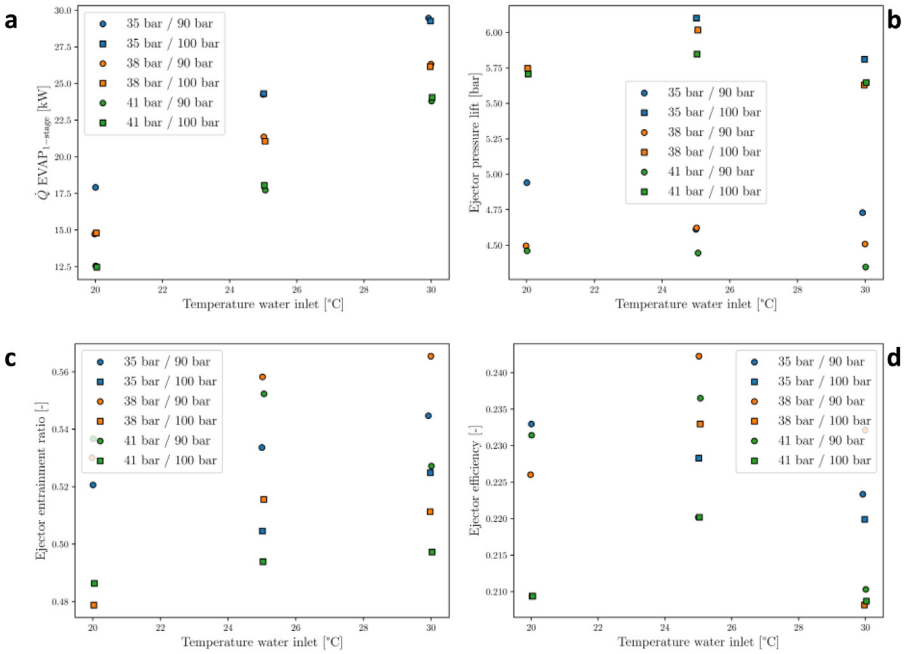

Fig. B1. Results obtained in the test campaign with $EVAP_{1\text{-stage}}$ and LP ejector. The legend defines first the evaporator pressure (e.g., 35 bar) and then the ejector motive conditions, either 90 bar (35 °C) or 100 bar (40 °C). Water mass flow rate equal to 0.31 kg/s.

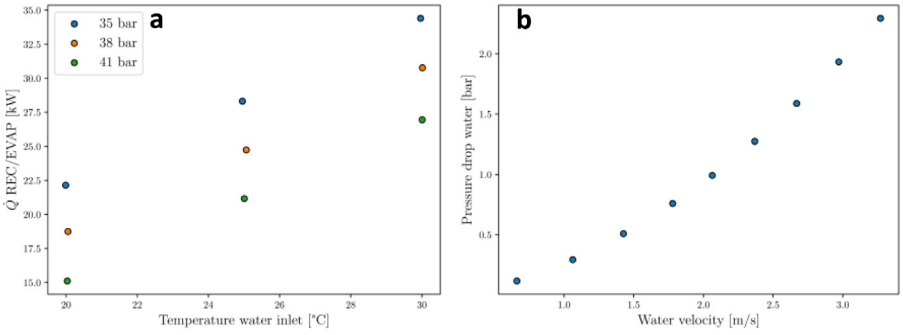

Fig. B2. Results obtained in the test campaign with the CO_2 receiver with evaporator submerged (REC/EVAP). a) heat flow rate as a function of evaporation pressure and water temperature at the inlet, with water mass flow rate equal to 0.31 kg/s. b) pressure drop in the water pipe as a function of water velocity.

the heat exchanger was sized for high water velocities (through the tube), to minimize biofouling formation and have an autocleaning effect. Thus, the pressure drop in the water side was quite relevant in this heat exchanger.

References

[1] IPCC, Climate change 2014: synthesis report, Intergovernmental Panel on Climate Change, Geneva, Switzerland, 2015.

[2] IEA, Technology and innovation pathways for zero-carbon-ready buildings by 2030, IEA, 2022. https://www.iea.org/reports/technology-and-innovation-pathways-for-zero-carbon-ready-buildings-by-2030/introduction.

[3] F. Meggers, H. Leibundgut, The potential of wastewater heat and exergy: Decentralized high-temperature recovery with a heat pump, Energ. Build. 43 (2011) 879–886, https://doi.org/10.1016/j.enbuild.2010.12.008.

[4] A. Cooperman, J. Dieckmann, Drain water heat recovery, ASHRAE J. 53 (2011) 58.

[5] J. Frijns, J. Hofman, M. Nederlof, The potential of (waste)water as energy carrier, Energ. Conver. Manage. 65 (2013) 357–363, https://doi.org/10.1016/j.enconman.2012.08.023.

[6] A. Mazhar, S. Liu, A. Shukla, A Key Review of Non-Industrial Greywater Heat Harnessing, Energies 11 (2018) 386, https://doi.org/10.3390/en11020386.

[7] IEA, Technology Roadmap. Energy-efficient Buildings: Heating and Cooling Equipment, 2011. https://www.iea.org/reports/technology-roadmap-energy-efficient-buildings-heating-and-cooling-equipment.

[8] Climate Action Tracker, Decarbonising Buildings-Achieving zero carbon heating and cooling, 2022. https://climateactiontracker.org/documents/1018/CAT_2022-03-09_Report_DecarbonisingBuildings.pdf.

[9] S.S. Cipolla, M. Maglionico, Heat recovery from urban wastewater: Analysis of the variability of flow rate and temperature, Energ. Build. 69 (2014) 122–130, https://doi.org/10.1016/j.enbuild.2013.10.017.

[10] A. Hepbasli, E. Biyik, O. Ekren, H. Gunerhan, M. Araz, A key review of wastewater source heat pump (WWSHP) systems, Energ. Conver. Manage. 88 (2014) 700–722, https://doi.org/10.1016/j.enconman.2014.08.065.

[11] L. Ni, S.K. Lau, H. Li, T. Zhang, J.S. Stansbury, J. Shi, J. Neal, Feasibility study of a localized residential grey water energy-recovery system, Appl. Therm. Eng. 39 (2012) 53–62, https://doi.org/10.1016/j.applthermaleng.2012.01.031.

[12] A. Kahraman, A. Çelebi, Investigation of the Performance of a Heat Pump Using Waste Water as a Heat Source, Energies 2 (2009) 697–713, https://doi.org/10.3390/en20300697.

[13] J. Wallin, J. Claesson, Analyzing the efficiency of a heat pump assisted drain water heat recovery system that uses a vertical inline heat exchanger, Sustain. Energy Technol. Assess. 8 (2014) 109–119, https://doi.org/10.1016/j.seta.2014.08.003.

[14] S. Chao, J. Yiqiang, Y. Yang, D. Shiming, W. Xinlei, A field study of a wastewater source heat pump for domestic hot water heating, Build. Services Eng. Res. Technol. 34 (2013) 433–448, https://doi.org/10.1177/0143624412463571.

[15] S. Chao, J. Yiqiang, Y. Yang, D. Shiming, Experimental performance evaluation of a novel dry-expansion evaporator with defouling function in a wastewater source heat pump, Appl. Energy 95 (2012) 202–209, https://doi.org/10.1016/j.apenergy.2012.02.030.

[16] C. Shen, L. Yang, X. Wang, Y. Jiang, Y. Yao, An experimental and numerical study of a de-fouling evaporator used in a wastewater source heat pump, Appl. Therm. Eng. 70 (2014) 501–509, https://doi.org/10.1016/j.applthermaleng.2014.05.055.
[17] C. Shen, Y. Jiang, Y. Yao, X. Wang, An experimental comparison of two heat exchangers used in wastewater source heat pump: A novel dry-expansion shell-and-tube evaporator versus a conventional immersed evaporator, Energy 47 (2012) 600–608, https://doi.org/10.1016/j.energy.2012.09.043.
[18] European Commission, Regulation (EU) No 517/2014 of the European Parliament and of the Council of 16th April 2014 on fluorinated greenhouse gases and repealing Regulation (EC) No 842/2006, 2014.
[19] UNIDO, The Montreal Protocol evolves to fight climate change, (2016).
[20] R.A. Otón-Martínzez, F. Illán-Gómez, J.R. García-Cascales, F.J. Sánchez-Velasco, V. Sena-Cuevas, External water subcooling to improve the performance of a CO2 heat pump for water heating that uses greywater as heat source, in: Proceedings of the 18th International Refrigeration and Air Conditioning Conference at Purdue, May 24-28, 2021, n.d.
[21] I.H. Bell, J. Wronski, S. Quoilin, V. Lemort, Pure and Pseudo-pure Fluid Thermophysical Property Evaluation and the Open-Source Thermophysical Property Library CoolProp, Ind. Eng. Chem. Res. 53 (2014) 2498–2508, https://doi.org/10.1021/ie4033999.
[22] J. Dusek, K. Skacanova, N. Masson, C. Mao, Global trends for CO2 heat pumps – A study of market, technology and policy drivers in Japan, China, North America and Europe., 2015. doi:10.18462/IIR.ICR.2015.0822.
[23] S. Elbel, N. Lawrence, Review of recent developments in advanced ejector technology, Int. J. Refrig. 62 (2016) 1–18, https://doi.org/10.1016/j.ijrefrig.2015.10.031.
[24] X. Cao, X. Liang, L. Shao, C. Zhang, Performance analysis of an ejector-assisted two-stage evaporation single-stage vapor-compression cycle, Appl. Therm. Eng. 205 (2022), https://doi.org/10.1016/j.applthermaleng.2021.118005.
[25] T. Bai, G. Yan, J. Yu, Thermodynamics analysis of a modified dual-evaporator CO2 transcritical refrigeration cycle with two-stage ejector, Energy 84 (2015) 325–335, https://doi.org/10.1016/j.energy.2015.02.104.
[26] G. Tosato, S. Girotto, S. Minetto, A. Rossetti, S. Marinetti, An integrated CO_2 unit for heating, cooling and DHW installed in a hotel. Data from the field, J. Phys. Conf. Ser. 1599 (2020), https://doi.org/10.1088/1742-6596/1599/1/012058.
[27] P. Artuso, G. Tosato, A. Rossetti, S. Marinetti, A. Hafner, K. Banasiak, S. Minetto, Dynamic Modelling and Validation of an Air-to-Water Reversible R744 Heat Pump for High Energy Demand Buildings, Energies 14 (2021) 8238, https://doi.org/10.3390/en14248238.
[28] L. Zheng, J. Deng, Experimental investigation on a transcritical CO2 ejector expansion refrigeration system with two-stage evaporation, Appl. Therm. Eng. 125 (2017) 919–927, https://doi.org/10.1016/j.applthermaleng.2017.07.056.
[29] P. Nekså, H. Rekstad, G.R. Zakeri, P.A. Schiefloe, CO2-heat pump water heater: characteristics, system design and experimental results, Int. J. Refrig. 21 (1998) 172–179, https://doi.org/10.1016/S0140-7007(98)00017-6.
[30] G. Lorentzen, Revival of carbon dioxide as a refrigerant, Int. J. Refrig. 17 (1994) 292–301, https://doi.org/10.1016/0140-7007(94)90059-0.
[31] G. Boccardi, F. Botticella, G. Lillo, R. Mastrullo, A.W. Mauro, R. Trinchieri, Experimental investigation on the performance of a transcritical CO2 heat pump with multi-ejector expansion system, Int. J. Refrig. 82 (2017) 389–400, https://doi.org/10.1016/j.ijrefrig.2017.06.013.
[32] S. Minetto, R. Brignoli, K. Banasiak, A. Hafner, C. Zilio, Performance assessment of an off-the-shelf R744 heat pump equipped with an ejector, Appl. Therm. Eng. 59 (2013) 568–575, https://doi.org/10.1016/j.applthermaleng.2013.06.032.
[33] S. Elbel, Historical and present developments of ejector refrigeration systems with emphasis on transcritical carbon dioxide air-conditioning applications, Int. J. Refrig. 34 (2011) 1545–1561, https://doi.org/10.1016/j.ijrefrig.2010.11.011.
[34] T. Bai, G. Yan, J. Yu, Thermodynamic analyses on an ejector enhanced CO2 transcritical heat pump cycle with vapor-injection, Int. J. Refrig. 58 (2015) 22–34, https://doi.org/10.1016/j.ijrefrig.2015.04.010.
[35] S. Elbel, P. Hrnjak, Experimental validation of a prototype ejector designed to reduce throttling losses encountered in transcritical R744 system operation, Int. J. Refrig. 31 (2008) 411–422, https://doi.org/10.1016/j.ijrefrig.2007.07.013.
[36] Y. Zhu, Y. Huang, C. Li, F. Zhang, P.-X. Jiang, Experimental investigation on the performance of transcritical CO2 ejector–expansion heat pump water heater system, Energ. Conver. Manage. 167 (2018) 147–155, https://doi.org/10.1016/j.enconman.2018.04.081.
[37] B.R. Brodie, Y. Takano, M. Gocho, Evaporator with Integrated Ejector for Automotive Cabin Cooling, in: 2012: pp. 2012-01–1048. doi:10.4271/2012-01-1048.
[38] A. Makoto Ikegami, T. Hiroshi Oshitani, Etsuhisa Yamada, O. Naohisa Ishizaka, N. Hirotsugu Takeuchi, A. Takeyuki Sugiura, T. Takuo Maehara, Ejector cycle system, US 8,991,201 B2, 2015.
[39] A. Hafner, Integrated CO2 system for refrigeration, air conditioning and sanitary hot water., (2017). doi:10.18462/IIR.NH3-CO2.2017.0015.
[40] M.M. Hazarika, J. Bengsch, J. Hafsas, A. Hafner, E.S. Svendsen, Z. Ye, Integration of gravity-fed evaporators in CO2 based heat-pump chillers., (n.d.). doi:10.18462/IIR.GL2022.0091.
[41] A. Hafner, M.M. Hazarika, F. Lechi, A. Zorzin, A.A. Pardiñas, K. Banasiak, Experimental investigation on integrated two-stage evaporators for CO2 heat-pump chillers., (n.d.). doi:10.18462/IIR.GL2022.0237.
[42] Alfa Laval, AXP brazed plate heat exchangers, (n.d.). https://www.alfalaval.com/products/heat-transfer/plate-heat-exchangers/brazed-plate-heat-exchangers/axp/ (accessed August 24, 2022).
[43] N. Lawrence, S. Elbel, Experimental Investigation on Control Methods and Strategies for Off-Design Operation of the Transcritical R744 Two-phase Ejector Cycle, Int. J. Refrig. (2019), https://doi.org/10.1016/j.ijrefrig.2019.04.020.
[44] P. Kalinski, The Danfoss Multi Ejector range for CO_2 refrigeration: design, applications and benefits, 2019.
[45] S. Coşkun, A.R. Motorcu, N. Yamankaradeniz, E. Pulat, Evaluation of control parameters' effects on system performance with Taguchi method in waste heat recovery application using mechanical heat pump, Int. J. Refrig. 35 (2012) 795–809. doi:10.1016/j.ijrefrig.2011.12.008.
[46] J. Claesson, Correction of logarithmic mean temperature difference in a compact brazed plate evaporator assuming heat flux governed flow boiling heat transfer coefficient, Int. J. Refrig. 28 (2005) 573–578, https://doi.org/10.1016/j.ijrefrig.2004.09.011.
[47] M.-H. Kim, J. Pettersen, C.W. Bullard, Fundamental process and system design issues in CO2 vapor compression systems, Prog. Energy Combust. Sci. 30 (2004) 119–174, https://doi.org/10.1016/j.pecs.2003.09.002.
[48] JCGM, Evaluation of measurement data—Guide to the expression of uncertainty in measurement, 2008.
[49] C. Aprea, F. de Rossi, R. Mastrullo, The uncertainties in measuring vapour compression plant performances, Measurement 21 (1997) 65–70, https://doi.org/10.1016/S0263-2241(97)00040-7.
[50] D. Gorenflo, S. Kotthoff, Review on pool boiling heat transfer of carbon dioxide, Int. J. Refrig. 28 (2005) 1169–1185, https://doi.org/10.1016/j.ijrefrig.2005.09.008.
[51] J.R. Thome, G. Ribatski, State-of-the-art of two-phase flow and flow boiling heat transfer and pressure drop of CO2 in macro- and micro-channels, Int. J. Refrig. 28 (2005) 1149–1168, https://doi.org/10.1016/j.ijrefrig.2005.07.005.
[52] J. Pettersen, Flow vaporization of CO2 in microchannel tubes, Exp. Therm. Fluid Sci. 28 (2004) 111–121, https://doi.org/10.1016/S0894-1777(03)00029-3.
[53] P. Gullo, B. Elmegaard, G. Cortella, Energy and environmental performance assessment of R744 booster supermarket refrigeration systems operating in warm climates, Int. J. Refrig. 64 (2016) 61–79, https://doi.org/10.1016/j.ijrefrig.2015.12.016.